Materials Advances

ROYAL SOCIETY OF CHEMISTRY

PAPER

View Article Online
View Journal | View Issue

Cite this: *Mater. Adv.*, 2024, 5, 2316

Deposition of multilayer coatings onto highly porous materials by Layer-by-Layer assembly for bone tissue engineering applications using cyclic mechanical deformation and perfusion

MohammadAli Sahebalzamani,[abc] Tina Sadat Hashemi,[abf] Zohreh Mousavi Nejad,[ab] Srishti Agarwal,[ab] Helen O. McCarthy,[d] Tanya J. Levingstone[abcfhi] and Nicholas J. Dunne *[abcdefghi]

By using Layer-by-Layer (LbL) assembly, micro- and nano-scale coatings can be applied to porous structures, allowing for the potential customisation of scaffolds for bone tissue engineering applications. In this study, we developed a purpose-designed LbL assembly system, enabling continuous perfusion flow and cyclic compression, to fabricate LbL multilayer-coated scaffolds with tailored properties. Their physicochemical properties were analysed using SEM and FTIR spectroscopy, while their elastic compressive modulus quantified their mechanical performance. This study compared immersion alone (*i.e.*, static conditions) to the combination of perfusion flow (12 mL min^{-1}, 10 rpm) and cyclic compressive loading (5% strain, 1 Hz) (*i.e.*, dynamic conditions) as methods to influence coating deposition during LbL assembly. The results demonstrated that the LbL-coated scaffolds with 40-multilayer coatings deposited under dynamic conditions demonstrated a 40-fold improvement in the compressive elastic modulus compared to uncoated scaffolds and a 16-fold increase was achieved when the LbL coatings were applied under static conditions. Importantly, application of the dynamic coating conditions during the LbL assembly process preserved the high porosity and interconnectivity of the scaffolds even after applying the 40-multilayer coating. Moreover, the nanocomposite coatings enhanced surface characteristics such as roughness and hydrophilicity. Taken together, adoption of the proposed approach of combining perfusion flow and cyclic compression loading during assembly of LbL-coated scaffolds is a promising approach for bone tissue engineering applications.

Received 4th September 2023,
Accepted 18th December 2023

DOI: 10.1039/d3ma00664f

rsc.li/materials-advances

Introduction

Various methods, such as autografts, allografts, and synthetic biomaterial-based bone grafts, are used to repair bone defects.[1,2] However, autologous and allografts have certain clinical limitations.[3] To overcome these limitations, tissue-engineered bone scaffolds and synthetic biomaterial bone grafts are being explored and are gaining popularity.[4,5] Bone scaffold materials play a crucial role in facilitating bone repair by providing a supportive framework for cellular attachment, proliferation, and new tissue formation.[6] However, effective fabrication is challenging, as these grafts need to mimic the osteogenesis of native tissue with interconnected porosity while meeting structural, mechanical, and biological requirements.[6,7] Nanomaterials and nanocoatings offer a new strategy for functionalising and tailoring bone substitute materials to achieve the required mechanical properties and porosity.[8] The development of nanoscale-film manufacturing technologies has opened new possibilities for surface modification of biomimetic scaffolds, which mimic the natural bone structures and extracellular matrices.[9] These scaffolds have been shown to promote cell proliferation and migration, aiding tissue regeneration.[10] Techniques such as the Langmuir–Blodgett method, self-assembled monolayers, and Layer-by-Layer (LbL) assembly have been used in the fabrication of ultra-thin films.[11]

LbL assembly presents an exciting opportunity to modify both the surface and bulk properties of bone-tissue-engineered

[a] *School of Mechanical and Manufacturing Engineering, Dublin City University, Ireland*
[b] *Centre for Medical Engineering Research, Dublin City University, Ireland*
[c] *Biodesign Europe, Dublin City University, Ireland*
[d] *School of Pharmacy, Queen's University Belfast, Belfast BT9 7BL, UK*
[e] *Department of Mechanical and Manufacturing Engineering, School of Engineering, Trinity College Dublin, Ireland*
[f] *Advanced Manufacturing Research Centre (I-Form), School of Mechanical and Manufacturing Engineering, Dublin City University, Ireland*
[g] *Advanced Materials and Bioengineering Research Centre (AMBER), Trinity College Dublin, Ireland*
[h] *Advanced Processing Technology Research Centre, Dublin City University, Ireland*
[i] *Trinity Centre for Biomedical Engineering, Trinity Biomedical Sciences Institute, Trinity College Dublin, Ireland*

scaffolds.[12] The LbL assembly process, a template-assisted deposition technique, is used for fabricating thin film layers and functionalizing surfaces.[13] It involves the sequential adsorption of oppositely charged electrolyte complexes onto a substrate, resulting in a uniform multilayer thin film.[13,14] Nanocomposite coatings deposited using LbL assembly can be used to tailor the mechanical properties and biofunctionality of scaffolds, including controlled release of therapeutic agents, biodegradability, improved biocompatibility, and cell and protein attachment, for repairing bone defects.[13,15] Thin films using LbL assembly have been deposited through dip coating, spray coating, and spin coating.[16] However, coating porous scaffolds with LbL assembly is challenging.[17] Spray and spin coatings are more suitable for flat surfaces and may result in uneven coatings on porous scaffold surfaces, leaving surfaces deeper in the scaffold without coating materials.[18,19] Dip-coating/immersion has traditionally been used in bone tissue engineering to fabricate films on porous scaffolds. Scaffolds are submerged in a solution containing the coating material, which adsorbs onto the scaffold surface *via* electrostatic interactions (Fig. 1).[20,21] However, for highly porous scaffolds, the coating solution may be rapidly absorbed, leading to non-uniform coatings. This variation in coating thickness and composition negatively affects the performance of LbL-coated materials.[13] Furthermore, submerging porous scaffolds in solutions or during washing cycles can generate air bubbles within cellular structures, adversely impacting the mechanical properties.[22,23]

An adapted dipping technique, whereby a continuous perfusion flow system is used to deliver solutions into the scaffold, has been employed to address the challenges associated with coating a porous scaffold through LbL assembly.[8,24,25] A perfusion flow system provides greater control over the coating process, optimising parameters like flow rate, pressure, and exposure duration to the coating solution, enabling strategic uniform coating deposition and resulting in improved uniformity and quality.[19,26,27]

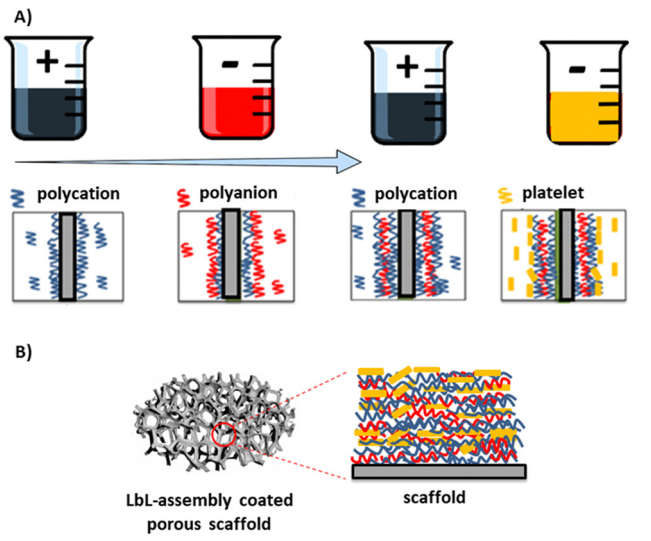

Fig. 1 Schematic of the LbL-assembly technique applied to highly porous scaffolds for bone tissue engineering applications. (A) Representation of the LbL-assembly process. (B) Changes of the scaffold surface after the LbL-assembly coating.

The application of mechanical deformation during the LbL assembly process has been shown to positively affect the physicochemical and mechanical properties of polymer-nanocomposite–coated bone scaffolds due to their localisation in highly deformed areas.[28,29] Ziminska *et al.* previously enhanced the physical and mechanical properties of LbL assembly coatings,[12,30] showing that polymer-based porous scaffolds coated with 60 multilayers exhibited increased mass and bulk elastic moduli of 2.5 MPa compared to 0.1 MPa when uncoated. Albro *et al.* demonstrated that applying dynamic loading at 1 Hz and 10% compressive strain amplitudes to a deformable porous agarose hydrogel-based scaffold enhanced solute transport within the scaffold.[31] In hydrated polymers, the application of cyclic loading has been shown to enhance the diffusion rate of large molecules compared to passive diffusion.[32]

Mechanical deformation enables thicker coatings to be deposited on areas of porous scaffolds experiencing higher loading, leading to a synthetic form of mechanical adaptation (similar to Wolff's law in bone) and improved mechanical performance.[28,33] Previous studies have demonstrated enhanced bone cell proliferation, differentiation and matrix deposition in response to combined perfusion flow with mechanical deformation.[34,35] Despite the substantial literature on LbL assembly covering a wide range of topics,[13] the effect of dynamic loading conditions and perfusion flow on the growth of LbL-assembled films has not been explored. This research delves into an innovative approach, focusing on the application of dynamic coating conditions within the LbL assembly process. This study is the first to evaluate the changes in the physical and mechanical properties of nanocomposite–coated 3D porous scaffolds fabricated using a combination of cyclic compressive loading and perfusion flow during the LbL assembly process. The primary aim of this study was to develop a purpose-designed deposition system capable of applying continuous perfusion flow and cyclic compression loading during the LbL assembly process. Furthermore, this study aimed to analyse the effects of both stimuli on the fabrication of nanocomposite coatings for application in bone tissue engineering scaffolds. Additionally, this study incorporated a novel composite coating system into the LbL assembly process. Previous research has not explored the use of porous templates for bone tissue scaffolds with this material-based approach.

Materials and methods

Materials system

Polymer-nanocomposite films were fabricated using LbL assembly with polyelectrolyte solutions of poly-L-lysine monohydrochloride (PLL), poly-L-glutamic acid (PGA), poly(diallyldimethylammonium chloride) (PDDA), and montmorillonite nanoclay (MTM). The addition of these biopolymers in LbL coatings enhances adhesion and stability, and provides control over coating thickness and composition. The MTM nanoclay, known for its low cost,

biocompatibility, and exceptional in-plane elastic modulus, is used to reinforce the mechanical properties of the polymer films.[12,30,33]

PLL powder (Mw: 182.65 g mol^{-1}), PGA powder (Mw: 147.13 g mol^{-1}), and PDDA solution (Mw: 400 kDa, 20 wt% in H_2O) were purchased from Sigma-Aldrich (UK). The MTM (Cloisite Na^+) was obtained from Blagden Chemicals Ltd, UK. Aqueous solutions of 1 wt% PLL, 1 wt% PGA and 1 wt/vol% PDDA were prepared by diluting them in deionised water under vigorous stirring conditions for 12 h. The pH of the resulting PDDA solution was approximately 5.5 and was not adjusted. The pH of the resulting PLL solution was adjusted from 6 to 4 by adding 0.1 M HCl, and the pH of the resultant PGA solution was adjusted from 5 to 7 by adding 0.5 M NaOH. Aqueous solutions of 0.5 wt% MTM clay were prepared by diluting them in deionised water under vigorous stirring conditions for 24 h. The pH of the MTM solution was 9.5 and was not adjusted.

Due to its biocompatibility, low cost, and similar porosity and pore size to cancellous bone, open-cell polyurethane (PU) foam was selected as the 3D porous template.[33,36] PU foam is commonly used as a scaffold-based material for the evaluation of orthopaedic devices, as a cancellous core material in bone models,[30,37] and for LbL assembly applications.[13,38] Cylindrical specimens measuring 10 mm in diameter and 12 mm in height were cut from PU foam sheets with 30 pores per inch (PPI) and 97% porosity (EasyFoam Ltd, UK) using a 12 mm circular surgical biopsy punch (Acuderm Inc. USA). Each specimen was cleaned in a 1 M NaOH solution for 10 min to remove unwanted debris and then rinsed with DI water. Each specimen was then placed in a desiccator and allowed to dry for 24 h before deposition.

Design and fabrication of the LbL deposition system

This study introduces a novel LbL assembly system that emulates Wolff's law for the fabrication of porous scaffolds. This allows for the development of lightweight synthetics with exceptional load-bearing capabilities and high porosity.[28] By applying mechanical deformation during the LbL assembly process, thicker coatings can be selectively deposited in areas of porous scaffolds experiencing higher loads.[12] To accurately represent *in vivo* conditions, the perfusion system's flow rates and compression-induced strain rates were carefully chosen.[39] A custom LbL deposition chamber, designed using SolidWorks 2020 software (DS SolidWorks Corp., USA) and manufactured thereafter (Fig. 2A and B), enabled simultaneous compression and perfusion flow during the deposition process.

The deposition equipment consisted of a bespoke deposition chamber containing the porous scaffold, connected to a plunger for solution pumping. A stepper motor applied the actuation force *via* the plunger to compress the scaffold. Custom software and an Arduino (IDE, 1.8.15) controlled the stepper motor, automating the compression cycles. Peristaltic pumps (323S/D, Watson-Marlow, UK) regulated the solution flow into the chamber. The LbL assembly system can accommodate up to four different solutions, pumping them simultaneously and alternately. The exposure time of each scaffold to solutions or rinse cycles was precisely controlled to 1 s. To measure the force exerted by the motor and control the force acting on the scaffold, a load cell (Flexiforce, Parallax Inc., USA) was positioned between the stepper plate and the plunger. Validation ensured uniform and reproducible loading, crucial for generating comparable results across different runs. Fig. 2C illustrates the force level produced at 10 rpm during a 30 s coating period. The peak loads remained constant throughout the test, with a maximum force of 0.239 N $\pm$ 0.011 and a minimum force of 0.089 N $\pm$ 0.024, resulting in a range of 0.158 N $\pm$ 0.122.

To investigate the effect of cyclic mechanical deformation and perfusion flow on coating deposition rates, porous scaffolds were coated under either static conditions where no loading was applied or dynamic conditions where cyclic mechanical deformation was applied with a compressive strain amplitude of 0.5 mm and a frequency of 1 Hz[12] throughout the LbL assembly process using the purpose-designed deposition apparatus.

LbL assembly procedure

Each scaffold was placed in a sealed chamber to fabricate a porous nanocomposite material and subjected to alternating solutions of oppositely charged species to produce a nanocomposite thin film under dynamic coating conditions. Each coating layer, referred to as a Quadlayer (QL), was produced by exposure to four electrolyte-based solutions: (i) a 1 wt% PLL solution with a positive charge, (ii) a 1 wt% PGA solution with a negative charge, (iii) a 1 wt% PDDA solution with a positive charge and (iv) a 0.5 wt% MTM nanoclay solution with a negative charge. The coating deposition process was conducted *via* the LbL assembly method using the purpose-design deposition chamber under a perfusion flow system and compression (a compressive strain amplitude of 0.5 mm and a frequency of 1 Hz) (Fig. 2D). Each solution was delivered into the deposition chamber for 30 s at a flow rate of 12 mL min^{-1}, which is similar to the flow rates that have previously been shown to promote bone growth within bioreactor systems,[32,39,40] while simultaneously draining the deposition chamber. The volume of each solution was equal to the chamber volume, approximately 7 mL. Between the introduction of each solution, the deposition chamber was rinsed for 30 s using deionised water as described by Ziminska *et al.* and Podsiadlo *et al.*[12,41] After the deposition of every 10 QLs, the coated scaffold was removed from the deposition chamber, rinsed three times with deionised water, and dried in a desiccator for 24 h. The process was repeated to deposit additional QLs until reaching the desired number of QLs. A minimum of 40 QLs was chosen as the starting point to detect significant differences in the investigated properties. The deposition chamber and exit tubing were cleaned and dried after each scaffold was coated with 10 QLs.

Under the static coating conditions, an immersion coating technique was applied, whereby the specimens were coated with 40 QLs by immersing the substrates in alternating solutions (each for 30 s) to mimic the LbL assembly conditions in a controlled-flow chamber. The solutions (PLL, PGA, PDDA, and MTM nanoclay) were placed in 500 mL beakers, and three rinsing beakers containing DI H_2O were used. The solutions and the water-containing beakers were changed after each 10 QL deposition. Macroscopic images of the uncoated scaffold and LbL coated scaffold following the deposition of 40-

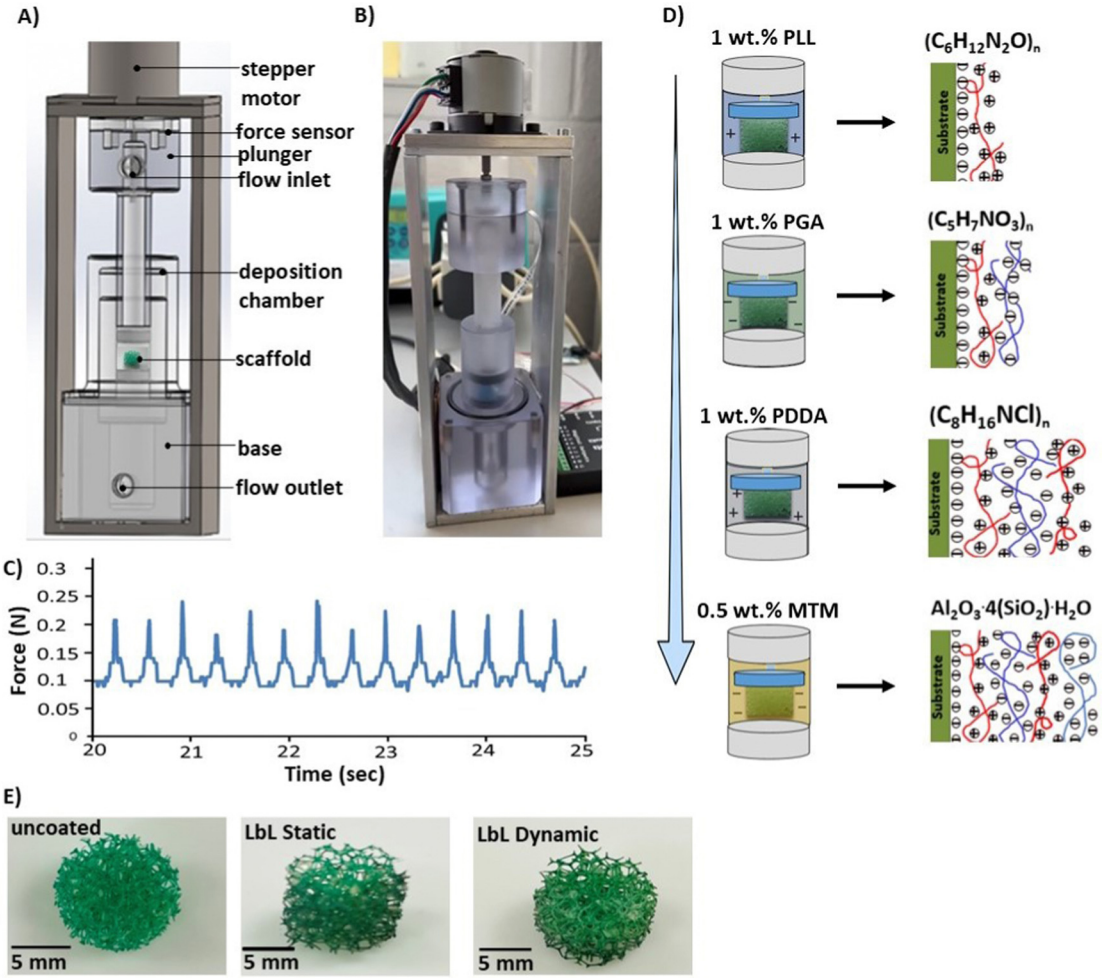

Fig. 2 Custom designed LbL deposition chambers and the process of applying multilayer coatings on 3D porous scaffold templates. (A) SolidWorks design and (B) manufactured purpose-designed deposition chambers capable of demonstrating perfusion-compression strain during the LbL assembly process. (C) Typical force wave generated during one coating period with a compressive strain amplitude of 0.5 mm and a frequency of 1 Hz with repeatable and constant force peaks. (D) Schematic demonstrating the LbL assembly process of multilayer coating onto a 3D porous scaffold template by perfusion flow of electrolyte solutions and cyclic compression using the purpose-designed deposition chamber. (E) Macroscopic images of the uncoated scaffold [(10 mm × 12 mm) with 30 pores per inch (PPI) and 97% porosity] and LbL-coated scaffolds following the deposition of 40-multilayer nanocoating under static and dynamic conditions.

multilayer nanocoating under static and dynamic conditions are presented in Fig. 2E.

Chemical characterisation

Fourier-transform infrared (FTIR) spectroscopy was conducted using a PerkinElmer Spectrum 100 instrument (PerkinElmer, Inc., USA) to investigate the chemical composition of each scaffold. Spectra ranging from 550 to 4000 cm^{-1} were acquired, with an average of 64 scans per spectrum. To enable the convenient comparison of multiple peaks, the transmission values of the FTIR spectra were adjusted. Characteristic functional groups were identified by examining the absorbance ranges of analogous organic and inorganic compounds.

Gravimetric analysis

Gravimetric analysis was used to investigate the variation in the mass of the LbL coating under different coating conditions. After the deposition of every 5 PLL/PGA/PDDA/MTM QLs, the weight of each coated scaffold was measured using an analytical balance with a resolution of 0.0001 g. Prior to weighing, each scaffold was maintained under ambient conditions (approximately 23 °C and 30% relative humidity) for a minimum of 8 h. The recorded mass was obtained by averaging five measurements.

Coating morphology and thickness

The morphology and coating thickness of each PLL/PGA/PDDA/MTM-coated scaffold were determined as a function of the number of QLs deposited using SEM. ImageJ software (version 1.44p, National Institutes of Health, USA) was used for image analysis. The coating thickness was calculated by measuring 10 data points from at least four SEM images captured at different locations on each sample.

Surface roughness

The surface roughness of each scaffold was quantified using a TR200 surface profilometer (Beijing TIME High Technology

Ltd, China.) in accordance with ISO 4287 : 1997.[42] The roughness average (Ra) was measured for each scaffold, which represents the arithmetic mean of the absolute values of the profile heights over the evaluation length.

Water contact angle

To assess the hydrophobicity of each scaffold before and after the coating assembly process, contact angle analysis was conducted, considering the inherent hydrophobic nature of the PU-based scaffolds. The dynamic contact angle was determined using the sessile drop method, involving the placement of one 5 μL droplet of water on the scaffold surface, followed by the measurement of the contact angle using a contact measuring device (FTÅ200 Dynamic Contact Angle Analyser, First Ten Angstroms, Inc., USA).

Porosity

To evaluate the influence of the coating on the overall scaffold porosity, the percentage porosity of the scaffold was calculated before and after undergoing the coating assembly process (eqn (1)). The apparent density (ρ_{apparent}) of the scaffold was determined using the gravimetric method, employing a Sartorius LA 620P Toploader scale balance (Sartorius Ltd, UK) with a YDL01 density determination kit. The maximum theoretical density (ρ_{maximum}) of the PU foam scaffold was 1.20 g cm^{-3}.[43]

$$\text{Porosity}(\%) = \left(\left(1 - \frac{\rho_{\text{apparent}}}{\rho_{\text{maximum}}}\right) \times 100\right) \quad (1)$$

Mechanical properties

The compressive properties of each scaffold coated with PLL/PGA/PDDA/MTM were measured using a CellScale Univert Universal Testing Machine (CellScale, Canada). A 50 N load cell was used to apply a 0.6 mm deflection to each scaffold at a crosshead speed of 0.5 mm min^{-1}, with a preload of 10 N. Each compression test was continued to failure, and a stress *vs.* strain plot was recorded. The compressive elastic modulus was determined by identifying the maximum slope within the linear region of the stress *vs.* strain plot, immediately after the toe region.

Statistical analysis

The data were presented as the mean ± standard deviation, based on five replicates for each analysis for each sample group. Prior to conducting statistical analysis, the homogeneity of variance was assessed. To analyse the dependencies, independent sample *t*-tests were used, with statistical significance set at $p < 0.05$. Five different samples were randomly selected from each test group for each characterisation method.

Results

Chemical characterisation

The chemical composition of the LbL-assembled coating was confirmed by acquiring the FTIR spectra (Fig. 3A). Spectra were collected for uncoated scaffolds and LbL-coated scaffolds fabricated under static and dynamic conditions. In the case of 40 QL-coated scaffolds prepared using both conditions, the chemical bonds remained consistent, and characteristic peaks confirmed the presence of individual PLL/PGA/PDDA/MTM nanoclay components, as outlined in Table 1.[44–46] Comparing the LbL-assembled coatings produced under static and dynamic conditions, stronger chemical bonds were observed in the latter, as indicated by the peaks used to identify functional groups. This can be attributed to the more compact and uniform coating achieved using the dynamic coating conditions.

Gravimetric analysis

Gravimetric analysis, a versatile and time-tested analytical method, is applicable to reaction systems of any scale and uniformity. This method allows for the determination of the average growth of the specimen (QL deposition) by measuring the change in the specimen mass.[47] In this study, scaffolds deposited under both static and dynamic conditions exhibited a consistent increase in mass with the number of QLs of PLL/PGA/PDDA/MTM deposited (Fig. 3B). Notably, LbL-coated scaffolds under dynamic conditions displayed a significantly higher mass ($p < 0.05$) compared to those coated under static conditions. Specifically, for the LbL-coated scaffold, the mass increased by 18.90 ± 1.56 mg following the deposition of 40 QLs under dynamic conditions, while under static conditions, it increased by 8.31 ± 2.74 mg.

Multilayer coating thickness

To ensure the uniformity and consistency of the coating in the LbL process, an analysis of the coating thickness was performed using SEM. Fig. 3C illustrates the average thickness of the multilayer coating obtained under both static and dynamic conditions. The results indicated that for 40 QLs, the coating thickness increased by 5.74 ± 1.89 μm under dynamic conditions and 4.21 ± 1.36 μm under static conditions.

SEM images of the cross-sections of the LbL-coated scaffolds exhibited a conformal coating that completely covered the substrate, with a noticeable increase in thickness in line with the gravimetric analysis findings (Fig. 4a–f). Upon closer examination at higher magnification, the layered structure of the LbL coatings was clearly observed as anticipated, along with the discernible edges of the nanoclay sheets integrated into the coating as expected (Fig. 4g and h).

Surface roughness

Rougher surfaces can mimic the cellular microenvironment found in nature, offering physical and chemical cues that enhance cell adhesion and function.[48,49] In the case of LbL-coated scaffolds, the Ra profile parameters were found to be higher when compared to the uncoated scaffolds. However, this increase was not deemed statistically significant due to the high variance in the data recorded for each sample tested (Table 2).

Water contact angle

The contact angle serves as an important determinant of the macroscopic wettability of a solid surface and plays a vital role

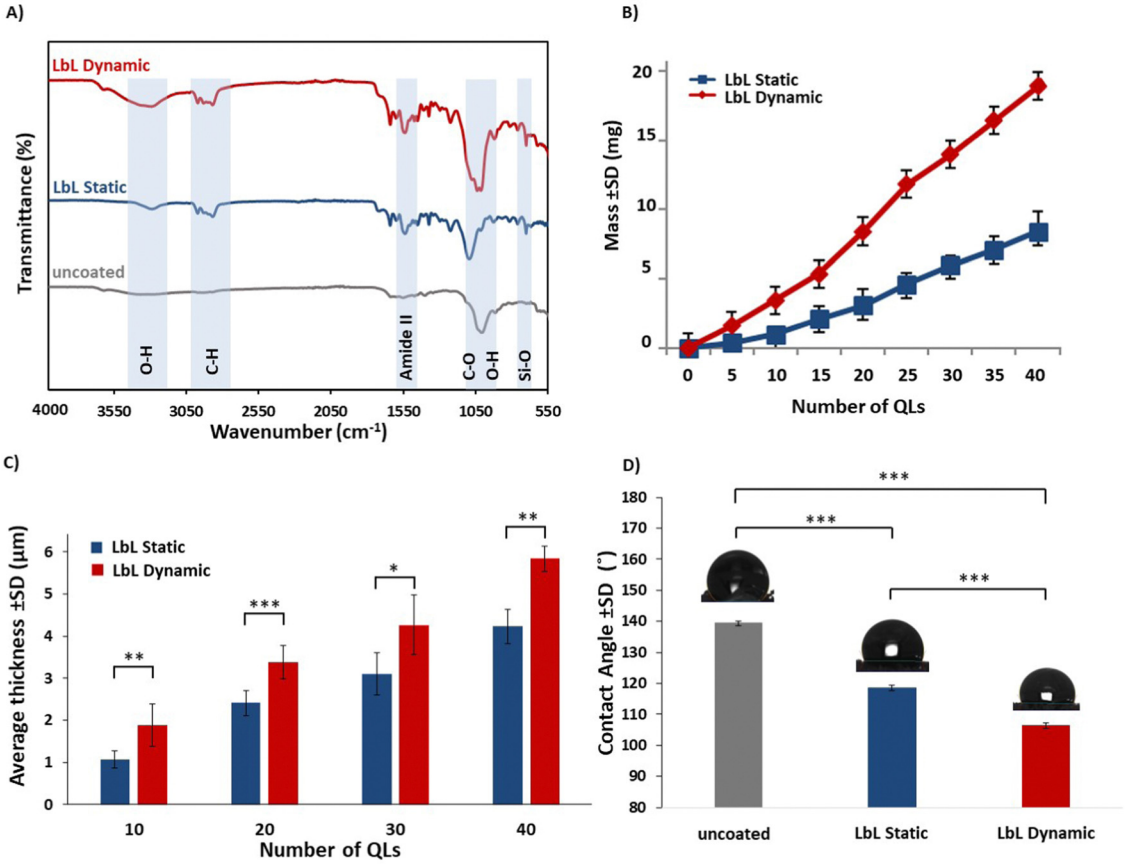

Fig. 3 Experimental data for the uncoated scaffolds and scaffolds coated using LbL deposition under static (LbL static) and dynamic conditions (LbL dynamic). The LbL-coated scaffolds had a coating of 40 QLs unless otherwise stated. (A) The FTIR spectra demonstrating characteristic peaks for the presence of individual PLL/PGA/PDDA/MTM nanoclay components, with the shaded region indicating distinct peaks associated with different levels of functional groups. (B) Gravimetric data: mean mass (± SD) of uncoated scaffolds and scaffolds coated under static and dynamic conditions. (C) Average thickness of the LbL-coating after 10, 20, and 40 QLs as measured using SEM. (D) Mean contact angle measurement. The values are presented as the mean ± standard deviation (n = 5). *$p < 0.05$, **$p < 0.01$, ***$p < 0.001$.

Table 1 FTIR spectra peaks and functional groups assigned

Wavenumber (cm^{-1})	Functional group
3350	O–H stretching
2800	–C–H stretching of $–CH_2$ of protein
1550	Amide II linkage
1050	C–O stretching/O–H deformation
700	Si–O stretching

in understanding the interfacial interactions between a solid and a liquid.[50,51] Fig. 3D illustrates the contact angles of both the uncoated and LbL-coated scaffolds. The uncoated scaffolds exhibited a contact angle of 139.57 ± 1.86°, whereas the LbL-coated scaffolds, fabricated under static and dynamic conditions, displayed contact angles of 118.73 ± 3.14° and 105.48 ± 2.23°, respectively. The differences in contact angles between the uncoated and LbL-coated scaffolds suggested that the incorporation of MTM nanoclay enhanced the hydrophilicity of the scaffolds. Moreover, the adoption of the dynamic LbL coating approach resulted in greater hydrophilicity, which has the potential to promote positive cellular interactions thus enhancing its efficacy in biomedical applications such as in bone tissue engineering where the specific attachment of the target cell type to the scaffold is required for optimal healing and regeneration.[52] Furthermore, the introduction of a hydrophilic substrate can be beneficial for the promotion of protein adhesion for drug delivery systems.[53]

Porosity

Highly porous scaffolds with interconnected pore structures are highly desirable for applications in bone tissue engineering as the porous architecture plays a critical role in promoting cell attachment, proliferation, and differentiation.[54] In our study, the uncoated scaffolds displayed an initial porosity of 97.40 ± 0.70% with a pore distribution range of 119–581 µm. While the LbL-coated scaffolds fabricated under static and dynamic conditions exhibited reduced porosities of 81.10 ± 0.45% and 86.20 ± 0.72%, and pore size distribution ranges of 110–429 µm and 114–476 µm. These findings indicate that the LbL assembly process effectively maintained the highly porous and interconnected architecture of the scaffold irrespective of the process conditions. Notably, increasing the number of layers in the LbL-assembled coating has the potential to offer several advantages for bone

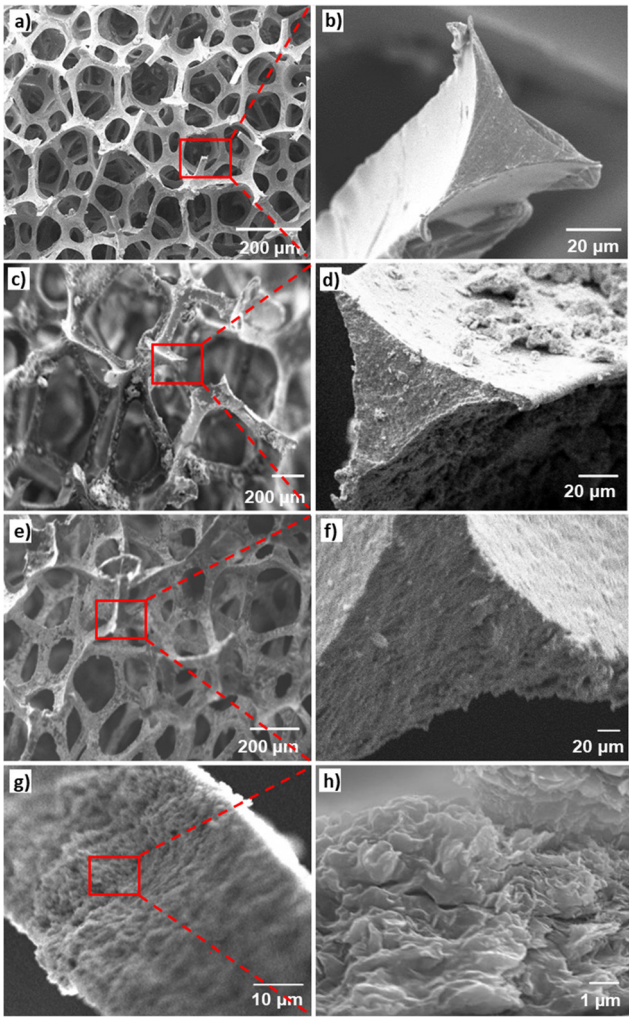

Fig. 4 SEM images of uncoated and LbL-coated scaffolds coated with 40 QLs. (a) and (b) SEM images of uncoated scaffolds. (c) and (d) SEM images of the LbL-coated scaffold fabricated under static conditions. (e) and (f) SEM images of the LbL-coated scaffold fabricated under dynamic conditions. (g) Dense multilayers within a cross-section of the LbL-coating fabricated under dynamic conditions. (h) Evidence of the successful integration of nanoclay sheets within the LbL-coating fabricated under dynamic conditions.

tissue engineering applications. Specifically, increased nanoclay deposition has the potential to improve the mechanical properties, while incorporating additional layers of the amino acid components (PLL and PGA) within the LbL-assembled coating could enhance cellular interaction and biocompatibility.[55] This flexibility enables the design of the LbL-assembled coating to be tailored to match the requirements for specific bone tissue engineering applications.

Mechanical properties

The mechanical behaviour of both uncoated scaffolds and LbL-coated scaffolds, fabricated under static and dynamic conditions, was significantly ($p < 0.05$) influenced by the presence of the PLL/PGA/PDDA/MTM coating, as evident from the representative stress *vs.* strain plots (Fig. 5A and B). The compressive elastic modulus of the uncoated scaffolds exhibited a significant enhancement for 40 QLs coated scaffolds. The modulus increased from 0.09 ± 0.05 MPa to 1.45 ± 0.41 MPa (16-fold increase) when the LbL coating was applied under static conditions and to 3.65 ± 0.70 MPa (40-fold increase) under dynamic conditions. Therefore, the custom designed LbL system significantly enhanced the mechanical performance of coated scaffolds under dynamic conditions compared to that under static conditions using immersion. The improvement achieved under dynamic conditions was more than double that observed under static conditions.

Discussion

The field of bone tissue engineering has witnessed significant advancements in recent years, with the emergence of effective bone scaffold materials that enhance bone healing in cases where natural healing is insufficient.[56,57] Scaffolds with a high degree of open pores that are interconnected offer increased surface area for cell–material interaction and facilitate efficient nutrient and waste exchange.[49] In this study, the 40-multilayer LbL-coated scaffold, fabricated under dynamic coating conditions, maintained a highly porous (≈ 86%) and interconnective structure with a pore size distribution ranging from 114 to 474 μm. Consequently, the physical properties and architecture of the scaffold remained uncompromised following the LbL process, and potentially provides a suitable platform for bone tissue engineering applications.[58,59] To understand the cell–material interaction of the optimal LbL-coated scaffold, *in vitro* biological assessment is required.

To optimise the performance of porous bone scaffolds in bone tissue engineering applications, the utilisation of the LbL assembly technique presents a versatile and precise method for tailoring their surface properties and enhancing their physio-mechanical properties.[8,21] However, conventional methods of coating such scaffolds using LbL assembly methods encounter challenges due to the difficulty in effectively infiltrating the coating materials into the porous structure.[24,33] Previous studies have attempted to address this issue by modifying the assembly process or introducing additives to enhance coating penetration.[12,58] Consequently, there is a pressing need for innovative approaches that can address these challenges and improve the outcomes of bone

Table 2 Mean ± standard deviation surface roughness of scaffolds (n = 5)

Scaffold type	Mean roughness, Ra (μm)
Uncoated	0.084 ± 0.044
LbL-coated scaffolds fabricated under static conditions	0.908 ± 0.125
LbL-coated scaffolds fabricated under dynamic conditions	1.56 ± 0.763

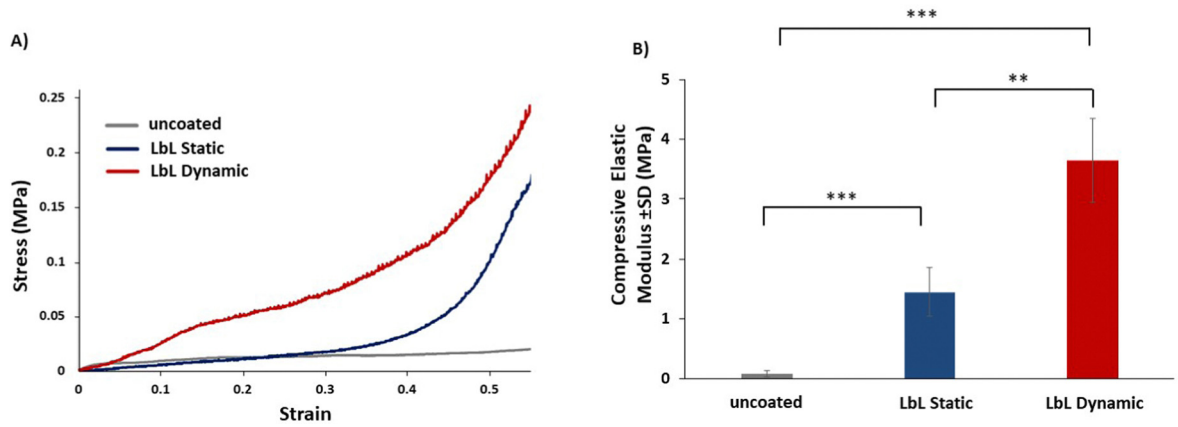

Fig. 5 Experimental mechanical testing was conducted to compare the mechanical properties of uncoated scaffolds with scaffolds coated using LbL deposition under static (LbL static) and dynamic (LbL dynamic) conditions. The LbL-coated scaffolds were uniformly coated with 40 QLs. (A) Typical stress *vs.* strain plots resulting from mechanical testing. (B) Mean elastic modulus (± SD) determined from the linear region of the plot, immediately after the toe region. The values are presented as the mean ± standard deviation (n = 5). *$p < 0.05$, **$p < 0.01$, ***$p < 0.001$.

tissue engineering. Given the limited research available in the existing literature regarding this specific aspect, the objective of this study was to investigate and develop an effective LbL assembly technique for the fabrication of highly porous scaffolds for use in bone tissue engineering applications. In this study, we explored the potential of applying dynamic coating conditions using the LbL assembly technique for fabricating micro/nanoscale coatings on porous scaffolds with the desired physio-mechanical and microarchitectural properties necessary for bone tissue engineering.

The materials used in this study PLL/PGA/PDDA/Na-MTM are known to be biocompatible and exhibit excellent suitability for tissue engineering applications. Through the technique of LbL assembly, these materials can be effectively combined to create coatings that enhance the mechanical properties and biocompatibility of bone scaffolds, making them highly promising for use in bone tissue engineering approaches.[12,13,30]

In this study, we present a novel approach that addresses the limitations of conventional methods by applying both perfusion flow and cyclic compression during the LbL deposition of polymer-nanocomposite coatings onto highly porous scaffolds. By applying dynamic LbL coating conditions during the assembly process, the diffusion of polyelectrolyte chains and nanoclay solutions into and out of the coating film can be facilitated, enabling the fabrication of ultrathin coating layers onto open-cell scaffolds.[12,30,58] This method not only improves the uniformity and thickness of the coatings but also has the potential to enhance their mechanical properties.[33] The purpose-designed LbL assembly system used in this study provides several advantages when compared to conventional methods.[11,59,60] It allows for precise control over perfusion flow, enables the application of cyclic mechanical loading, and prevents coating solution deprivation, thereby eliminating air bubbles and the need for squeezing to remove previous coating solutions.[13]

Our results demonstrate several significant findings regarding the PLL/PGA/PDDA/Na-MTM nanoclay-based LbL-coated scaffolds fabricated under dynamic conditions. First, LbL-coated scaffolds fabricated under dynamic conditions exhibited stronger chemical bonding due to the uniform and homogeneous dispersion of the nanocomposite coating.[8,31,41] Moreover, LbL-coatings applied under dynamic conditions indicated faster growth rates of mass, denser, and more uniform coatings compared to coatings fabricated under static conditions. This is attributed to the improved penetration of the coating materials into the porous scaffold structure, leading to a higher coating mass and better coverage.[33] SEM analysis confirms these observations, revealing the superior coating morphology achieved under dynamic conditions. These findings are consistent with previous research where the application of cyclic mechanical loading during the LbL assembly has been shown to enhance the diffusion of polyelectrolytes and result in thicker coatings.[12] These results therefore emphasize the significance of cyclic deformation in promoting the formation of thicker coatings. Despite the increased coating thickness resulting from the dynamic coating conditions, the scaffolds maintained a high porosity and an interconnected pore structure that resembles the trabecular structure of naturally spongy bone.

Furthermore, improvement in the wettability and surface roughness of the LbL-coated scaffolds fabricated under dynamic conditions offers additional advantages for bone tissue engineering.[49] These findings of increased surface roughness and decreased contact angle of LbL-coated scaffolds align with several studies that have highlighted the importance of surface characteristics in influencing cell behaviour on biomaterials.[51,61] The effect of the nanocomposite coatings on the surface properties of scaffolds has previously been shown to enhance cell adhesion and spreading.[13,62]

An important finding of this study was that the incorporation of nanoclays into the polymer–nanocomposite coatings significantly enhances their mechanical properties, resulting in coatings with highly dispersed nanosheets and exceptional stiffness. This finding aligns with previous studies by Ziminska *et al.*, Li *et al.*, and Podsiadlo *et al.* demonstrating the reinforcing effect of nanoclays on polymer matrices.[12,30,41] For

instance, in a similar study conducted by Ziminska *et al.*, a 22-fold increase (from 0.078 MPa to 1.736 MPa) in the compressive elastic modulus through the deposition of 40 QLs when applying LbL-assembled coatings composed of polyacrylic acid (PAA), polyethyleneimine (PEI), and nanoclay onto open-cell substrates[33] was observed. One notable advantage observed in our study was that a significant increase in scaffold stiffness was achieved when the LbL coating was applied under dynamic conditions as opposed to static conditions. Specifically, the deposition of 40 QLs resulted in a 40-fold increase in the compressive elastic modulus compared to the that of uncoated scaffolds. In contrast, when the LbL coating was applied under static conditions, the increase was 16-fold, thus highlighting the superiority of dynamic conditions in enhancing scaffold stiffness.

This pioneering study established a highly replicable and precise protocol for the creation of polymer–nanocomposite coatings on highly porous materials. Taken together, these results demonstrate that the application of LbL-assembled nanocomposite multilayered coating onto highly porous scaffolds under perfused compression conditions is an effective deposition method for bone tissue engineering applications.[13] While scaffolds with desirable properties for bone tissue engineering applications have been achieved, there is a need for further optimisation of the coating process conditions to achieve greater control over coating properties such as coating thickness and uniformity. Further research should prioritise investigating the influence of various LbL assembly process parameters on the physical, chemical, mechanical, and biological characteristics of LbL-coated porous scaffolds. To achieve this, a systematic parametric study could be designed to comprehensively evaluate and optimise these LbL assembly process parameters, aiming to attain the desired properties. As exemplified by the innovative design of the proposed novel LbL system investigated herein, it is possible to develop customised approaches to modulate the properties of porous LbL-coated scaffolds. Further optimisation of these LbL-coated porous scaffolds will not only establish a favourable microenvironment for cell adhesion and proliferation but also ensures the preservation of stable mechanical properties under hydrated conditions. Building on the improvements in the surface characteristics and physico-mechanical performance of the LbL-coated scaffolds fabricated under dynamic conditions, further work is needed to understand and validate the influence of combining perfusion flow and cyclic compression loading during the LbL assembly process. This validation requires *in vitro* biological assessments, specifically focusing on biocompatibility and ability to support cell adhesion, proliferation and differentiation – aspects that were not explored in this study.

Conclusions

The LbL assembly technique holds great promise for the fabrication of scaffolds for bone tissue engineering applications, offering a cost-effective and precise coating method that is compatible with various substrates, thus showcasing its high versatility. In this study, we developed a novel automated LbL assembly system that incorporates the application of perfusion flow and cyclic compressive loading during the deposition of PLL/PGA/PDDA/Na-MTM nanoclay-based LbL coatings on highly porous scaffolds, specifically for bone tissue engineering. LbL-assembled coatings fabricated under dynamic conditions were shown to offer significant advantages, with enhanced physical and mechanical characteristics compared to those fabricated under static conditions, where cyclic compressive loading was not applied. Scaffolds coated with PLL/PGA/PDDA/Na-MTM nanoclay-based LbL coatings deposited under dynamic conditions resulted in uniform and dense coatings that were thicker with stronger chemical bonding compared to scaffolds coated under static conditions. Additionally, the LbL-coated scaffolds coated under dynamic conditions showed a higher compressive elastic modulus and maintained a higher porosity compared to scaffolds coated under static conditions. Importantly, the novel LbL coating deposition method effectively preserved the highly porous and interconnective structure of the scaffold. In the context of surface properties, the LbL-coated scaffold fabricated under dynamic conditions exhibited enhanced surface hydrophilicity and surface roughness properties, both of which are considered important to facilitate effective cell and protein attachment. Overall, the adoption of combining perfusion flow and cyclic compression loading during assembly of LbL-coated scaffolds presents a promising approach for bone tissue engineering applications.

Data availability

Data will be made available upon request.

Conflicts of interest

There are no conflicts to declare.

Acknowledgements

The research conducted in this publication was funded by the Irish Research Council (Government of Ireland Scholarship Scheme) under award number GOIPG/2020/1344. The FTIR and contact angle analyses were carried at the Nano Research Facility (NRF) in Dublin City University (DCU), which was funded under the Programme for Research in Third Level Institutions (PRTLI) Cycle 5. The PRTLI is co-funded through the European Regional Development Fund (ERDF), part of the European Union Structural Funds Programme 2011–2015.

References

1 V. Georgeanu, O. Gingu, I. Antoniac and H. Manolea, Current Options and Future Perspectives on Bone Graft and Biomaterials Substitutes for Bone Repair, from Clinical Needs to Advanced Biomaterials Research, *Appl. Sci.*, 2023, **13**, 8471.

2 W. Wang and K. W. K. Yeung, Bone grafts and biomaterials substitutes for bone defect repair: A review, *Bioact. Mater.*, 2017, **2**(4), 224.
3 A. H. Schmidt, Autologous bone graft: Is it still the gold standard?, *Injury*, 2021, **52**, 18–22.
4 A. M. Tatara and A. G. Mikos, Tissue Engineering in Orthopaedics, *J. Bone Jt. Surg., Am.*, 2016, **98**(13), 1132.
5 A. Khademhosseini and R. Langer, A decade of progress in tissue engineering, *Nat. Protoc.*, 2016, **11**(10), 1775.
6 E. Chiarello, M. Cadossi, G. Tedesco, P. Capra, C. Calamelli and A. Shehu, *et al.*, Autograft, allograft and bone substitutes in reconstructive orthopedic surgery, *Aging: Clin. Exp. Res.*, 2013, **25**, 101–103.
7 S. Cao, Y. Zhao, Y. Hu, L. Zou and J. Chen, New perspectives: In-situ tissue engineering for bone repair scaffold, *Composites, Part B*, 2020, **202**, 108445.
8 S. Zhang, M. Xing and B. Li, Biomimetic Layer-by-Layer Self-Assembly of Nanofilms, Nanocoatings, and 3D Scaffolds for Tissue Engineering, *Int. J. Mol. Sci.*, 2018, **19**(6), 1641.
9 K. Ariga, E. Ahn, M. Park and B. S. Kim, Layer-by-Layer Assembly: Recent Progress from Layered Assemblies to Layered Nanoarchitectonics, *Chem. – Asian J.*, 2019, **14**(15), 2553.
10 Y. Gong, Y. Zhu, Y. Liu, Z. Ma, C. Gao and J. Shen, Layer-by-layer assembly of chondroitin sulfate and collagen on aminolyzed poly(L-lactic acid) porous scaffolds to enhance their chondrogenesis, *Acta Biomater.*, 2007, **3**(5), 677.
11 S. Park, U. Han, D. Choi and J. Hong, Layer-by-layer assembled polymeric thin films as prospective drug delivery carriers: design and applications, *Biomater. Res.*, 2018, **22**(1), 29.
12 M. Ziminska, M. J. Chalanqui, P. Chambers, J. Acheson, H. McCarthy and N. Dunne, *et al.*, Nanocomposite–coated porous templates for engineered bone scaffolds: A parametric study of layer-by-layer assembly conditions, *Biomed. Mater.*, 2019, **14**(6), 1–39.
13 A. Sahebalzamani, M. Ziminska, H. McCarthy, T. Levingstone, N. Dunne and A. Hamilton, Advancing Bone Tissue Engineering One Layer at a Time: Layer-by-Layer Assembly Approach to 3D Bone Scaffold Materials, *Biomater. Sci.*, 2022, 10.
14 M. Michel, V. Toniazzo, D. Ruch and V. Ball, Deposition Mechanisms in Layer-by-Layer or Step-by-Step Deposition Methods: From Elastic and Impermeable Films to Soft Membranes with Ion Exchange Properties, *Int. Scholarly Res. Not.*, 2012, 701695.
15 D. Alkekhia, P. T. Hammond and A. Shukla, Layer-by-Layer Biomaterials for Drug Delivery, *Annu. Rev. Biomed. Eng.*, 2020, **22**, 1–24.
16 N. M. Larocca, R. B. Filho and L. A. Pessan, Influence of layer-by-layer deposition techniques and incorporation of layered double hydroxides (LDH) on the morphology and gas barrier properties of polyelectrolytes multilayer thin films, *Surf. Coat. Technol.*, 2018, **349**, 1–12.
17 P. Nooeaid, W. Li, J. Roether, V. Mouriño, O. M. Goudouri and D. Schubert, *et al.*, Development of bioactive glass based scaffolds for controlled antibiotic release in bone tissue engineering via biodegradable polymer layered coating, *Biointerphases*, 2014, 9.
18 M. Salomäki, L. Marttila, H. Kivelä, M. Tupala and J. Lukkari, Oxidative Spin-Spray-Assembled Coordinative Multilayers as Platforms for Capacitive Films, *Langmuir*, 2020, **36**(24), 6736.
19 Z. Zhang, J. Zeng, J. Groll and M. Matsusaki, Layer-by-layer assembly methods and their biomedical applications, *Biomater. Sci.*, 2022, **10**(15), 4077.
20 S. Vozar, Y. C. Poh, T. Serbowicz, M. Bachner, P. Podsiadlo and M. Qin, *et al.*, Automated spin-assisted layer-by-layer assembly of nanocomposites, *Rev. Sci. Instrum.*, 2009, **80**(2), 023903.
21 O. Azzaroni and K. H. A. Lau, Layer-by-layer assemblies in nanoporous templates: nano-organized design and applications of soft nanotechnology, *Soft Matter*, 2011, **7**(19), 8709.
22 F. Carosio, F. Cuttica, A. D. Blasio, J. Alongi and G. Malucelli, Layer by layer assembly of flame retardant thin films on closed cell PET foams: Efficiency of ammonium polyphosphate versus DNA, *Polym. Degrad. Stab.*, 2015, **113**, 189.
23 Y. Pan, J. Zhan, H. Pan, W. Wang, G. Tang and L. Song, *et al.*, Effect of Fully Biobased Coatings Constructed via Layer-by-Layer Assembly of Chitosan and Lignosulfonate on the Thermal, Flame Retardant, and Mechanical Properties of Flexible Polyurethane Foam, *ACS Sustainable Chem. Eng.*, 2016, **4**(3), 1431.
24 J. Acheson, S. Goel, N. Dunne and A. Hamilton, Effect of hydration on the mechanical behaviour of nanocomposite–coated porous bone scaffold materials, 2015.
25 D. A. Garzón-Alvarado, M. A. Velasco and C. A. Narváez-Tovar, Modeling porous scaffold microstructure by a reaction-diffusion system and its degradation by hydrolysis, *Comput. Biol. Med.*, 2012, **42**(2), 147.
26 S. Yamada, M. A. Yassin, T. Schwarz, K. Mustafa and J. Hansmann, Optimization and Validation of a Custom-Designed Perfusion Bioreactor for Bone Tissue Engineering: Flow Assessment and Optimal Culture Environmental Conditions, *Front. Bioeng. Biotechnol.*, 2022, **10**, 811942.
27 C. F. Bellani, J. Ajeian, L. Duffy, M. Miotto, L. Groenewegen and C. J. Connon, Scale-Up Technologies for the Manufacture of Adherent Cells, *Front. Nutr.*, 2020, **7**, 575146.
28 M. Ziminska, A. Lennon, N. Dunne and A. Hamilton, Mimicking Wolff's law in synthetic porous materials: Mechanical behaviour of nanocomposite–coated foams fabricated under cyclic mechanical deformation: Bioengineering in Ireland 2018.
29 D. Mertz, J. Hemmerlé, J. Mutterer, S. Ollivier, J. C. Voegel and P. Schaaf, *et al.*, Mechanically responding nanovalves based on polyelectrolyte multilayers, *Nano Lett.*, 2007, **7**(3), 657.
30 M. Ziminska, N. Dunne and A. R. Hamilton, Porous Materials with Tunable Structure and Mechanical Properties via Templated Layer-by-Layer Assembly, *ACS Appl. Mater. Interfaces*, 2016, **8**(34), 21968.
31 M. B. Albro, N. O. Chahine, R. Li, K. Yeager, C. T. Hung and G. A. Ateshian, Dynamic loading of deformable porous media can induce active solute transport, *J. Biomech.*, 2008, **41**(15), 3152.
32 R. L. Mauck, C. T. Hung and G. A. Ateshian, Modeling of neutral solute transport in a dynamically loaded porous permeable gel: implications for articular cartilage biosynthesis and tissue engineering, *J. Biomech. Eng.*, 2003, **125**(5), 602.

33 M. Ziminska, N. Dunne and A. Hamilton, Customization of mechanical properties and porosity of bone tissue scaffold materials via Layer-by-Layer assembly of polymer-nanocomposite coatings, *MRS Online Proc. Libr.*, 2015, **1793**(1), 67–72.
34 M. V. Lipreri, N. Baldini, G. Graziani and S. Avnet, Perfused Platforms to Mimic Bone Microenvironment at the Macro/Milli/Microscale: Pros and Cons, *Front. Cell Dev. Biol.*, 2022, **9**, 760667.
35 J. Zhang, J. Griesbach, M. Ganeyev, A. K. Zehnder, P. Zeng and G. N. Schädli, *et al.*, Long-term mechanical loading is required for the formation of 3D bioprinted functional osteocyte bone organoids, *Biofabrication*, 2022, **14**(3), 035018.
36 P. S. D. Patel, D. E. T. Shepherd and D. W. L. Hukins, Compressive properties of commercially available polyurethane foams as mechanical models for osteoporotic human cancellous bone, *BMC Musculoskeletal Disord.*, 2008, **9**, 137.
37 J. A. Szivek, M. Thomas and J. B. Benjamin, Characterization of a synthetic foam as a model for human cancellous bone, *J. Appl. Biomater.*, 1993, **4**(3), 269.
38 Y. C. Li, Y. S. Kim, J. Shields and R. Davis, Controlling polyurethane foam flammability and mechanical behaviour by tailoring the composition of clay-based multilayer nanocoatings, *J. Mater. Chem. A*, 2013, **1**(41), 12987.
39 M. Jagodzinski, A. Breitbart, M. Wehmeier, E. Hesse, C. Haasper and C. Krettek, *et al.*, Influence of perfusion and cyclic compression on proliferation and differentiation of bone marrow stromal cells in 3-dimensional culture, *J. Biomech.*, 2008, **41**(9), 1885.
40 P. Godara, C. D. McFarland and R. E. Nordon, Design of bioreactors for mesenchymal stem cell tissue engineering, *J. Chem. Technol. Biotechnol.*, 2008, **83**(4), 408.
41 P. Podsiadlo, Z. Tang, B. S. Shim and N. A. Kotov, Counterintuitive effect of molecular strength and role of molecular rigidity on mechanical properties of layer-by-layer assembled nanocomposites, *Nano Lett.*, 2007, **7**(5), 1224.
42 B. Iso Geometric Product Specifications (GPS)—Surface texture: Profile method—Terms, definitions and surface texture parameters.
43 L. J. Gibson and M. F. Ashby, Cambridge Solid State Science Series, *Cellular Solids: Structure and Properties*, Cambridge University Press, Cambridge, 2nd edn, 1997, **https://www.cambridge.org/core/books/cellular-solids/BC25789552BAA8E3CAD5E1D105612AB5**.
44 S. Mazurek, A. Mucciolo, B. M. Humbel and C. Nawrath, Transmission Fourier transform infrared microspectroscopy allows simultaneous assessment of cutin and cell-wall polysaccharides of Arabidopsis petals, *Plant J. Cell Mol. Biol.*, 2013, **74**(5), 880.
45 B. Ludwig, Infrared Spectroscopy Studies of Aluminum Oxide and Metallic Aluminum Powders, Part II: Adsorption Reactions of Organofunctional Silanes, *Powders*, 2022, **1**(2), 75–87.
46 I. Notingher, J. Jones, S. Verrier, I. Bisson, P. Embanga and P. Edwards, *et al.*, Application of FTIR and Raman Spectroscopy to Characterisation of Bioactive Materials and Living Cells, *Spectrosc. Int. J.*, 2003, **17**, 275.
47 J. Byun, K. H. Kim, B. K. Kim, J. W. Chang, S. K. Cho and J. J. Kim, Gravimetric analysis of the autocatalytic growth of copper microparticles in aqueous solution, *RSC Adv.*, 2019, **9**(65), 37895.
48 B. Majhy, P. Priyadarshini and A. K. Sen, Effect of surface energy and roughness on cell adhesion and growth – facile surface modification for enhanced cell culture, *RSC Adv.*, 2021, **11**(25), 15467.
49 M. Mrksich, A surface chemistry approach to studying cell adhesion, *Chem. Soc. Rev.*, 2000, **29**(4), 267.
50 J. W. Song and L. W. Fan, Temperature dependence of the contact angle of water: A review of research progress, theoretical understanding, and implications for boiling heat transfer, *Adv. Colloid Interface Sci.*, 2021, **288**, 102339.
51 S. Cai, C. Wu, W. Yang, W. Liang, H. Yu and L. Liu, Recent advance in surface modification for regulating cell adhesion and behaviors, *Nanotechnol. Rev.*, 2020, **9**(1), 971.
52 A. K. Pearce and R. K. O'Reilly, Polymers for Biomedical Applications: The Importance of Hydrophobicity in Directing Biological Interactions and Application Efficacy, *Biomacromolecules*, 2021, **22**(11), 4459.
53 P. Kesharwani, A. Bisht, A. Alexander, V. Dave and S. Sharma, Biomedical applications of hydrogels in drug delivery system: An update, *J. Drug Delivery Sci. Technol.*, 2021, **66**, 102914.
54 H. R. R. Ramay and M. Zhang, Biphasic calcium phosphate nanocomposite porous scaffolds for load-bearing bone tissue engineering, *Biomaterials*, 2004, **25**(21), 5171.
55 M. Criado-Gonzalez, C. Mijangos and R. Hernández, Polyelectrolyte Multilayer Films Based on Natural Polymers: From Fundamentals to Bio-Applications, *Polymers*, 2021, **13**(14), 2254.
56 T. T. Roberts and A. J. Rosenbaum, Bone grafts, bone substitutes and orthobiologics: the bridge between basic science and clinical advancements in fracture healing, *Organogenesis*, 2012, **8**(4), 114.
57 M. Rupp, L. Klute, S. Baertl, N. Walter, G. K. Mannala and L. Frank, *et al.*, The clinical use of bone graft substitutes in orthopedic surgery in Germany-A 10-years survey from 2008 to 2018 of 1,090,167 surgical interventions, *J. Biomed. Mater. Res., Part B*, 2022, **110**(2), 350.
58 J. G. Acheson, A. McFerran, D. Xu, M. Ziminska, S. Goel and A. B. Lennon, *et al.*, Hydrated behavior of multilayer polyelectrolyte-nanoclay coatings on porous materials and demonstration of shape memory effect, *Surf. Coat. Technol.*, 2023, **458**, 129335.
59 C. Picart, J. Mutterer, L. Richert, Y. Luo, G. D. Prestwich and P. Schaaf, *et al.*, Molecular basis for the explanation of the exponential growth of polyelectrolyte multilayers, *Proc. Natl. Acad. Sci. U. S. A.*, 2002, **99**(20), 12531.
60 Z. Guo, M. Ziminska, A. D. Hamilton, C. McCoy and D. Sun, Multi-functional porous scaffold with LBL assembled

chitosan/graphene oxide nanocoating: Bioengineering in Ireland, 2018.
61 S. Metwally and U. Stachewicz, Surface potential and charges impact on cell responses on biomaterials interfaces for medical applications, *Mater. Sci. Eng., C*, 2019, **104**, 109883.
62 A. Ignatius, H. Blessing, A. Liedert, C. Schmidt, C. Neidlinger-Wilke and D. Kaspar, *et al.*, Tissue engineering of bone: effects of mechanical strain on osteoblastic cells in type I collagen matrices, *Biomaterials*, 2005, **26**(3), 311.